Journal of Solar Energy Research (JSER)

Journal homepage: jser.ut.ac.ir

Control of Three-Phase Buck-Type Dynamic Capacitor Using the Model Predictive Control Method for Dynamic Compensation of the Reactive Power and Load Current Harmonics

Vahid Souri [a], Abbas Ketabi[a*], Abolfazl Halvaei Niaser[a]

[a]*Department of Electrical Engineering, University of Kashan, Kashan, Iran*
[*]*Corresponding Author:* Abbas Ketabi, *E-mail Address:* aketabi@kashanu.ac.ir
Received: 26-11-2020
Accepted: 25-05-2021

Abstract

Dynamic capacitor (DCAP), as a shunt power quality device, corrects the power factor of the load and reduces the total harmonic distortion (THD) of the source current. A novel control method was presented based on the model predictive control (MPC) to control a three-phase three-wire buck-type DCAP. The injected current of DCAP is the control variable, which must be controlled by two power electronic switches of DCAP. MPC controller minimized the absolute value of the difference between a reference current and a DCAP current in the prediction horizon. The reference current consisted of two distinct parts, i.e., reactive power compensator (RPC), and harmonic current eliminator (HCE), based on the fundamental component of the load current. Also, a prediction model (PM) was proposed to calculate state variables of the DCAP based on their previous values, state of the switches, and prediction values of the grid voltage. The proposed PM was extracted from the linearized differential equations of the DCAP. All DCAP components, such as capacitors and inductors of the inner and outer filters, were modeled in the proposed PM. Unlike the PI controller, the proposed MPC has fewer control parameters and can use in extensive operational conditions. The simulation results in MATLAB software showed the superiority of the proposed method compared with the even harmonic modulation (EHM) method on a three-phase DCAP.

Keywords: Buck-Type Dynamic Capacitor (DCAP); Model Predictive Control (MPC); Reactive Power Compensator (RPC); Harmonic Current Eliminator (HCE).

1. INTRODUCTION

In the distribution systems, reactive power compensation and improvement of the power quality are considered as two important issues. Lack of reactive power injection on the load side can reduce power factor and voltage drop [1, 2]. Reactive power can be compensated statistically by installing a parallel capacitor bank, usually fixed on the load side or interfaced by mechanical switches [3]. However, these step capacitor banks are slow devices that are not suitable for accurate and rapid compensation of dynamic loads [4, 5]. Flexible alternating current transmission system (FACTS) devices are a convenient but expensive tool to compensate for these loads. For more than two decades, FACTS devices, currently used as the most important dynamic reactive power compensation equipment have been commercially available to power system operators.

Among these devices, static Var compensator (SVC) is more popular because it is simpler and cheaper and does not include an inverter, but SVC's response is slow to the loads with fast dynamics [6, 7].

The static synchronous compensator (STATCOM) has a DC/AC inverter with a high response speed. Therefore, it is very effective for applications where high response speeds are required for compensation [8-10]. However, this equipment is expensive to be used at medium and low voltage levels. On the other hand, specific features and requirements required for its DC link capacitor only make it possible for the electrolytic capacitor to meet such a requirement. The reliability of the STATCOM is influenced by the short life of these capacitors. However, studies have been performed on reducing the size of the capacitor or removing the DC link capacitor using AC/AC matrix converters [11, 12].

In addition to compensating for reactive power, the modern distribution system needs to eliminate harmonic loads. Nonlinear loads, such as diode and thyristor rectifiers inject large amounts of the current harmonics into the grid [13, 14]. Today, with the growth of power electronics, light and motor loads, formerly known as linear loads are changed through the addition of electronic power converters and act as nonlinear loads producing harmonic currents. Experience in utilizing the FACTS devices shows that many of these devices can be used in a multifunctional way (reactive and harmonic power compensation simultaneously) using appropriate control systems. Therefore, they are considered to be too expensive for use in low-voltage applications.

Dynamic capacitor (DCAP) was firstly introduced in 2010 as an integrated compensator for reactive and harmonic compensation by even harmonic modulation (EHM) method [15, 16]. DCAP is one of the new equipment offered to improve the quality of power. It is an economical solution with high reliability that does not require electrolytic capacitors. It consists of a power capacitor and a thin AC converter (TACC) that can be of buck, boost, or buck-boost topologies. DCAP, as a shunt power quality apparatus, is an economical but effective solution for dynamic reactive compensation. In the previous studies, for using DCAP, with a double-purpose buck-type design, a control method has been used based on the concept of virtual quadrature sources (VQS) and EHM, and proportional-integral (PI) controllers have been applied to compensate reactive and harmonic load capacity simultaneously [16, 17]. Regarding compensating for VAR based on the buck-type AC chopper, in a study [18], the relationship between the duty cycle of the switches and reactive compensation was extracted and injection current was controlled by a PI controller.

DCAP is equivalent to a variable capacitor in reactive power compensation performance and can cause series resonance if the grid voltage is harmonic. As in previous research, [19] quality of reactive current was improved to compensate for the power factor. In a study [20], DCAP control was used for a three-phase buck-type dynamic capacitor to prevent series resonance and improve the quality of injectable reactive flow. In the other studies [21, 22], DCAP control was performed by connecting the star in such a way that in addition to compensating for the unbalanced reactive power, it also compensated for load under light conditions. In a prior study [23], for achieving better performance in the three-phase buck-type DCAP and series and parallel resonance active damping, the analysis was performed to compensate for reactive power and harmonic suppression.

When DCAP acts as a reactive and harmonic compensator, duty cycle relation *D(t)* includes two parts, the DC part is used to regulate reactive current, and the harmonic part is used to regulate harmonic current. The main limitation is that D(t) must be chosen between 0 and 1. The interaction between reactive power compensation coefficients and harmonic elimination for DCAP was discussed in a previous study [24], and a flowchart was given to coordinate flow control.

Due to the interaction control loops at each frequency and the interaction between the fixed and harmonic parts of the duty cycle, DCAP control with PI controller based on the EHM method is very challenging and complex in all the studies. In the existing DCAP control method, only odd harmonics are compensated and it is not able to compensate for even harmonics. Also, the EHM method does not work well in the situations where voltage is harmonic at the point of common coupling PCC. Undoubtedly, the PI controller is one of the most popular controllers for linear systems. Therefore, the design method of PI controllers is too difficult for non-linear systems with limitations. These controllers are usually configured to achieve satisfactory performance only in a small

operating range, outside of which, performance deteriorates dramatically [25].

In recent years, model predictive control (MPC) has received a great deal of attention in the field of power electronics. MPC is capable of handling complex and nonlinear dynamics, and constraints can be explicitly included simply and effectively. There are two main MPC methods for power converters: (1) continuous control- set MPC (CCS-MPC) (2) finite-control-set MPC (FCS-MPC). In FCS-MPC, control objectives are evaluated by a cost function; the control set that minimizes the cost function is chosen as the optimal one and is applied in the next control period. FCS-MPC is a non-linear optimization control method and has good control and dynamic performance. FCS-MPC is simple in theory [26]. A significant advantage of the FCS-MPC is that control signals are applied directly to the system, and no modulator is required [27]. In general, MPC with a long forecast horizon has better performance in terms of stability than the MPC with a short horizon [25]. Therefore, in this paper, our proposed controller is based on the concept of FCS-MPC with a horizon greater than one sample. The proposed method is not influenced by the harmonic voltage of the grid and in the case where the point of common coupling (PCC) voltage is harmonic, the MPC method still compensates for reactive power and harmonics of the load.

The rest of the paper is organized into four sections: In Section 2, a state-space model of the DCAP is developed. MPC design is described in detail in Section 3. A discrete-time model is also presented for predicting values of the four DCAP state variables, reference current design, and MPC algorithm in this section. Finally, simulation and conclusion results are presented in Sections 4 and 5, respectively.

2. MODELING OF DCAP

2.1. Description of the System

Fig.1(a) shows per phase of the basic circuit structure of the buck type DCAP, consisting of *LC* input filter (L_F and C_F), buck-type thin AC converter (TACC), and power capacitor *C*. Input filter is used to suppress switching harmonics.

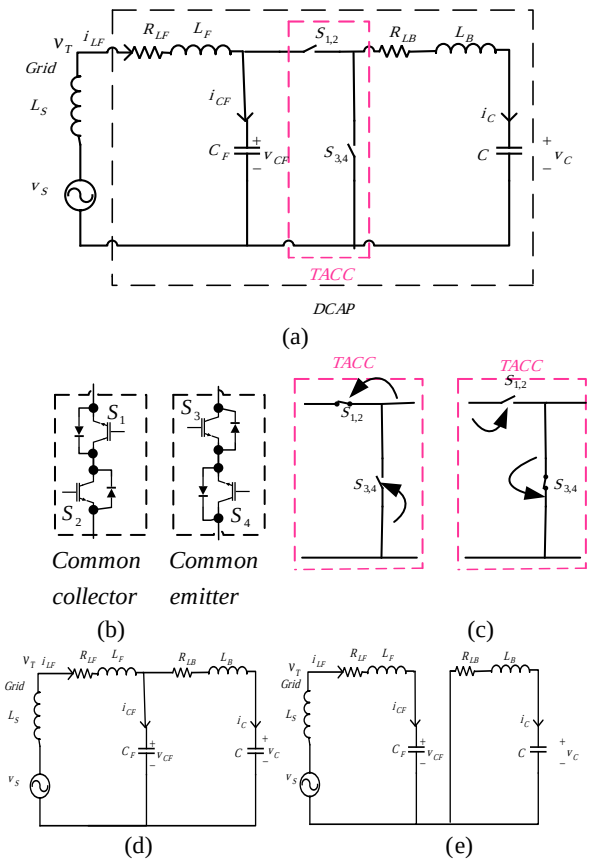

Fig.1 Buck DCAP (a) Circuit structure (b) Model switch (c) Two complementary switching modes (d) Equivalent circuit model in mode 1 (e) Equivalent circuit model in mode 2

Power capacitor is in series with a little buffer inductor L_B so that, inrush current could be restrained in case of turning-on or turning-off of switching devices of $S_{1,2}$ and $S_{3,4}$. DCAP has two switches including $S_{1,2}$ and $S_{3,4}$, whose command signals complement each other. Therefore, this converter has only two switching modes, as shown in Table 1, with a binary *S* variable. In mode 1 (S =1), switch $S_{1,2}$ is on, and switch $S_{3,4}$ is off. In mode 2 (S = 0), which is complementary to mode 1, $S_{3,4}$ is on, and the $S_{1,2}$ is off [19].

Table 1. Switching mode

S_1, S_2	S_3, S_4	Switching mode
ON	OFF	S=1
OFF	ON	S=0

2.2. State-Space Model of the DCAP

In Fig.1(a), it has been defined that $i_{LF}(t)$ is DCAP output current, $v_{CF}(t)$ is the voltage of filtering capacitor C_F, and $i_C(t)$ is the current of power capacitor C. Equations of an equivalent circuit of DCAP in time-domain of the presented circuit are expressed by Equations (1) - (4). The t index represents the time and i and v indicate the current and voltage of the elements, respectively. For example, $i_{CF,t}$, and $v_{CF,t}$ are the current and voltage of the capacitor C_F at time t, respectively.

$$i_{CF,t} = C_F \frac{dv_{CF,t}}{dt} \quad (1)$$

$$i_{C,t} = C \frac{dv_{C,t}}{dt} \quad (2)$$

$$v_{LB,t} = L_B \frac{di_{LB,t}}{dt} \quad (3)$$

$$v_{LF,t} = L_F \frac{di_{LF,t}}{dt} \quad (4)$$

According to the Kirchhoff's voltage law (KVL) and Kirchhoff's current law (KCL), equations of an equivalent circuit of DCAP are expressed by Equations (5) - (8). S_t is a binary variable showing switching mode at time t.

$$v_{CF,t} S_t = v_{C,t} + v_{LB,t} + R_{LB} i_{LB,t} \quad (5)$$

$$v_{S,t} = v_{LF,t} + R_{LF} i_{LF,t} + v_{CF,t} \quad (6)$$

$$i_{LF,t} = i_{CF,t} + i_{LB,t} S_t \quad (7)$$

$$i_{LB,t} = i_{C,t} \quad (8)$$

The variables of $v_{CF,t}$, $v_{C,t}$, $i_{LF,t}$, and $i_{LB,t}$ are the voltage across capacitors of C_F and C, and the current of inductors of L_F and L_B, respectively, and are considered as the four state variables of this converter. Equations (1) - (4) express the voltage-current relationship between capacitors of C_F and C, and inductors of L_F and L_B, respectively.

For the digital implementation of the power electronic circuits, it is necessary to use a discrete model to predict the future values of the state variables. Several convenient discretization methods are suitable for the calculation of predictions in the FCS-MPC. One of these methods is using the Euler approximation. If the derivative of the injected current into the grid is replaced by an Euler approximation in a sampling cycle, Equations (1) - (4) can be converted into the discrete form using Euler-approximation as follows:

$$i_{CF,k} = C_F \frac{v_{CF,k} - v_{CF,k-1}}{\Delta t} \quad (9)$$

$$i_{C,k} = C \frac{v_{C,k} - v_{C,k-1}}{\Delta t} \quad (10)$$

$$v_{LB,k} = L_B \frac{i_{LB,k} - i_{LB,k-1}}{\Delta t} \quad (11)$$

$$v_{LF,k} = L_F \frac{i_{LF,k} - i_{LF,k-1}}{\Delta t} \quad (12)$$

The k index represents the k^{th} time step and Δt also indicates the length of the time step. Discrete form of Equations (5) - (8) is shown in the Equations (13) - (16), respectively.

$$v_{CF,k} S_k = v_{C,k} + v_{LB,k} + R_{LB} i_{LB,k} \quad (13)$$

$$v_{S,k} = v_{LF,k} + R_{LF} i_{LF,k} + v_{CF,k} \quad (14)$$

$$i_{LF,k} = i_{CF,k} + i_{LB,k} S_k \quad (15)$$

$$i_{LB,k} = i_{C,k} \quad (16)$$

The four state variables of $v_{CF,k}$, $i_{LF,k}$, $v_{C,k}$, and $i_{LB,k}$ are calculated from their values in the last time step, i.e., $v_{CF,k-1}$, $i_{LF,k-1}$, $v_{C,k-1}$, and $i_{LB,k-1}$ by Equations (9) - (16) as expressed in the Appendix. The value of each of the state variables at time k must be calculated according to system inputs at time k, i.e., $v_{S,k}$ and S_k, as well as values of state variables in the previous step, $k-1$ to obtain a prediction model. The system of 8 equations with 8 non-linear unknowns expressed in Equations (9) -(16) is solved by the Symbolic math tool of the MATLAB software.

Equations (A1) - (A4) in the Appendix are called prediction model (PM). Using the model predictive, values of the four DCAP state variables in the k^{th} time step can be calculated using their corresponding values in the $(k-1)^{th}$ step, i.e., $v_{CF,k-1}$, $i_{LF,k-1}$, $v_{C,k-1}$, and $i_{LB,k-1}$. Therefore, the model predictive can be used to predict the values of state variables in steps $k+1$, $k+2$, ..., $k+n$, where n is the prediction horizon. For example, Fig.2 shows how to calculate the state variable in step k+1.

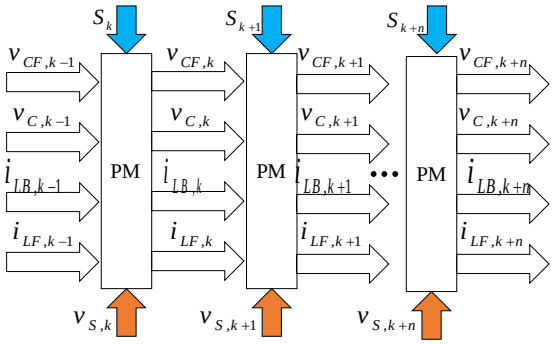

Fig.2 The model proposed for predicting DCAP state variables

In the presented prediction model, grid voltage must be predicted at all *n* moments. However, this prediction is possible due to the intermittent behavior of the voltage waveform. In this paper, it is assumed that voltage behavior in each cycle corresponds to its behavior in the previous cycle to predict the shape of the voltage wave at each step of the prediction horizon.

$$v_{S,k} = v_{S,k-P} \tag{17}$$

$$P = \frac{1}{f\,\Delta t} \tag{18}$$

In Eq. (17), *P* is the number of time steps making up a voltage cycle with frequency *f*. In the proposed predictor control, switching mode *S* is considered as a decision variable, the optimal value of which must be calculated on the prediction horizon. The approach for calculating switching mode S on the forward horizon will be presented in the next section.

3. FINITE CONTROL SET OF THE MODEL PREDICTIVE CONTROL

In the model predictive control given in this paper, the cost function is considered according to Eq.(19) as the sum of the absolute values of the difference between the reference current ($i^*_{LF,k}$) and DCAP ($i_{LF,k}$) current.

$$\min_{Duty} \; J = \sum_{z=k}^{k+n} \left| i_{LF,z} - i^*_{LF,z} \right| \tag{19}$$

Where, *J* is an objective function that must be minimized, where *z* and *n* indices are forward time step and prediction horizon, respectively. Decision variables are arranged in *n* duty vectors specifying the switching mode of *S* in the next time steps. This vector is described in the "Optimization" Section. As *n* increases, the computational burden of the predictive controller also increases. Therefore, a compromise should be made between the computational burden of the control system and the performance of the DCAP to determine *n*. When the value of the prediction horizon is selected equal to five switching cycles, grid current THD is less than 5%.

3.1. Determining the Reference Current

The reference current consists of two distinct parts, i.e., reactive power compensator (RPC) and harmonic current eliminator (HCE) that is calculated based on the fundamental component of the load current:

$$i^*_{LF,k} = i^{RPC*}_{LF,k} + i^{HCE*}_{LF,k} \tag{20}$$

The reference harmonic current eliminator includes the load current harmonic components and is determined as:

$$i^{HCE*}_{LF,k} = \left| i_{load,k} \right| \sin(\omega t + \angle i_{load,k}) - i_{load,k} \tag{21}$$

Where $\left| i_{load,k} \right|$ and $<i_{load,k}$ are the amplitude and angle of the fundamental component of load current in the k^{th} time step, respectively. The capacitor current fundamental component compensates the load current reactive part, and its amplitude is computed as:

$$i_{DCAP,k} = i_{load,k} \sin(\angle v_{T,k} - \angle i_{load,k}) \tag{22}$$

Where, $<v_{T,k}$ is the angle of the grid voltage in the k^{th} time step. Therefore, the reference reactive power current can be calculated as:

$$i^{RPC*}_{LF,k} = \left| i_{DCAP,k} \right| \sin(\omega t + \angle v_{T,k} + \frac{\pi}{2}) \tag{23}$$

Fig. 3 shows the block diagram of the DCAP reference current generation.

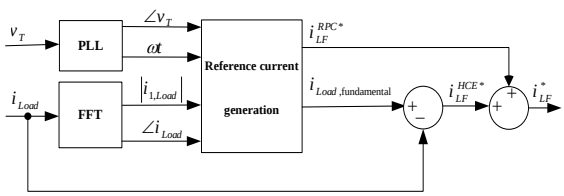

Fig. 3 Block diagram of the DCAP reference current generation

It should be noted that the amount of load current on the prediction horizon, as well as grid voltage, is

predicted using their corresponding values in the previous period:

$$i_{load,k} = i_{load,k-P} \tag{20}$$

Fig.4 shows a parallel connection per phase of buck-type DCAP and the proposed control system configuration with three-phase star-connected DCAP.

3.2. Optimization

In the proposed model predictive control method, optimization problem (19) must be solved at the beginning of each switching period to calculate the duty vector. According to Eq. (21), *duty* includes *b* vectors with *m* row of the D_i member.

$$Duty = \{D_1, ..., D_b\} \tag{21}$$

$$D_i = \{S_{(i-1)m+1}, ..., S_{(i-1)m+m}\} \tag{22}$$

Where *m* is the number of time steps making up a switching cycle with frequency f_s calculated by Eq.(23). D_i determines the status of the TACC switching in the *i-th* cycle, i.e., the time steps from $(i\text{-}1)_{m+1}$ to $(i\text{-}1)_{b+m}$.

$$m = \frac{1}{f_s \Delta t} \tag{23}$$

It should be noted that prediction horizon *n* must be chosen as an integer multiple of *m*:

$$n = b \times m \tag{24}$$

After determining *duty*, in the k[th] time step, D_1 is applied as switching mode in a switching cycle, i.e., in the k^{th} step up to $k+m-1$. The switching state, S, should be changed at most once in each switching period, so the constraint (25) is added to the optimization problem (19).

$$\sum_{z=1}^{m-1} \left| S_{(i-1)m+z} - S_{(i-1)m+z+1} \right| \le 1 \ \forall i \in \{1, ..., b\} \tag{25}$$

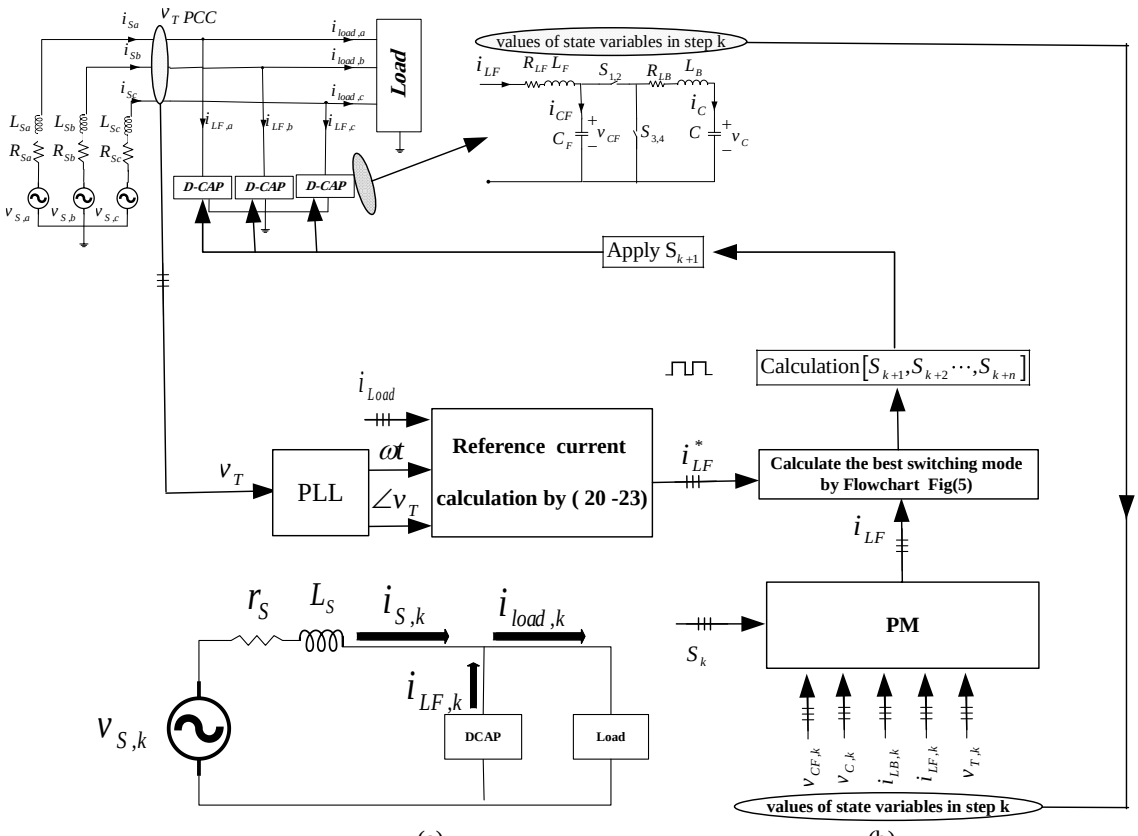

Fig.4 (a) Parallel connection per phase of buck-type DCAP (b) the proposed control system configuration with three-phase star-connected DCAP

Therefore, at the beginning of each switching cycle, switching vector D_1 must be determined by solving the optimization problem presented in Eq.(19). Admissible switching modes complying with Eq. (25) are first calculated and recorded in a switching table (*ST*) to determine the duty vector.

Steps of the proposed FCS-MPC method are as follows:

Step 1: Introduce the reference current and the predicted source voltage vectors

Step 2: Set *y*=0 and *Best=inf*.

Step 3: *For y*= 1: *Ymax*

Step 4: Calculate *J* by (19)

Step 5: *If J<Best*

Step 6: Set *Best=J* and $Duty_{best}=Duty$

Step 7: *End* of *If*.

Step 8: *End* of *For*

Step 9: Extract D_1 from $Duty_{best}$ using Eq. (21).Fig.5 presents the flowchart of the above steps. Where, $Duty_{best}$ is optimal duty response and *Ymax* is the number of all *duty* scheme in the *ST*.

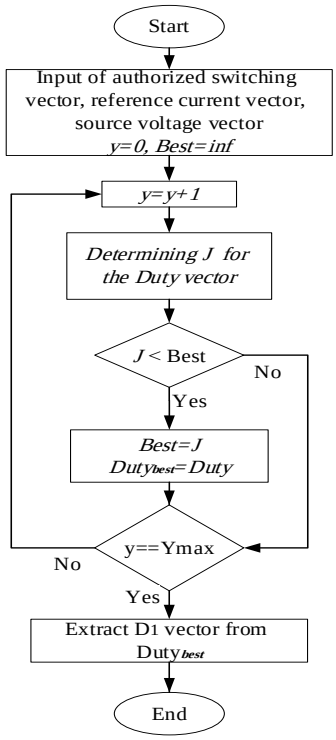

Fig.5 Flowchart of the duty-best determinant vector

4. SIMULATION RESULTS

A three-phase dynamic capacitor sample was tested simultaneously under lag and non-linear load, as shown in Fig.4 in the MATLAB environment to confirm the performance of the proposed MPC method in compensating for reactive power and capability of the harmonic filter. Grid voltage was assumed to be pure sinusoidal with an amplitude of 220 V at a frequency of 50 Hz. Parameters of the system and the LC filter were selected according to

Table2 [24]. Since, switching frequency was variable, so LC filter was selected based on the average switching frequency $f_{sw.av} \approx 12KHZ$.

The sampling time for discretization was *Ts* = 10μs, which can be implemented with DSP, TMS320 type [28] for example, and the sampling time for FCS-MPC execution is *5Ts*. Thus grid current harmonic distortion and power factor correction will meet the IEEE-STD519-1992 guidelines. The simulation results confirmed the validity of theoretical analysis as shown in Fig.6.

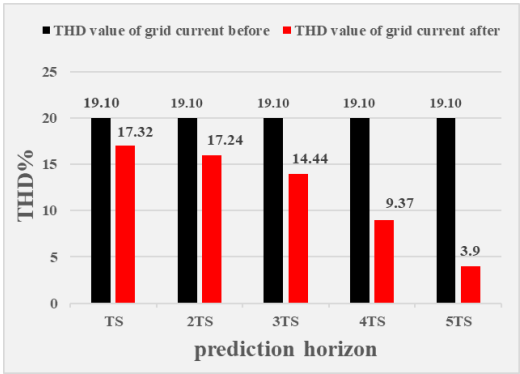

(a)

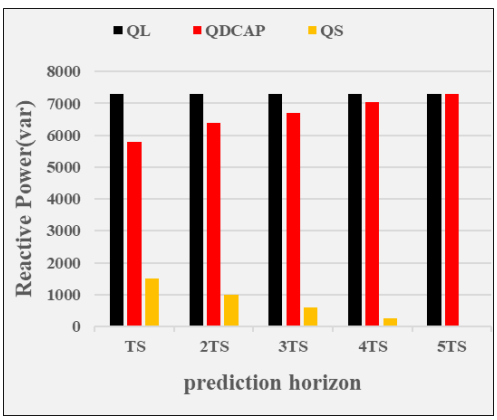

(b)

Fig.6 (a)The effect of prediction horizon before and after the presence of DCAP on THD value (b) The effect of prediction horizon on reactive power

Table2. Simulation parameters

Description	Parameter	Value
Grid voltage	Vs	$220V$
Frequency Grid	f	$50HZ$
grid inductance	L_S	$90\mu H$
power capacitor	C	$860\mu F$
Input filter inductance	L_F	$560\mu H$
Input filter capacitor	C_F	$80\mu F$
buffer inductance	L_B	$680\mu H$
Converter resistance	R_{LF}, R_{LB}	0.1Ω
linear load	L_L, R_L	$42.5mH$ 12.5Ω
non-linear load (DC-link inductor and resistor in series)	L_{dc}, R_{dc}	$200\mu H$ 18.7Ω

The buck-type DCAP was tested under three cases for compensation of reactive power and harmonic filter to verify the performance of the proposed control strategy, and the results of the proposed method were compared with those obtained using the EHM method. The first case occurred under lag and non-linear load with odd-order harmonics, the second case occurred under lag and non-linear load with odd and even -order harmonics, and the third case occurred when grid harmonic voltage and lag and non-linear load were drawn from the grid with odd-order harmonics.

4.1. Case 1

As shown in Fig.7 and Fig.8, the load current is lag and harmonic with the order of 13, and load current THD is equal to 19.10% while power factor is poor (0.89).

Fig.9 shows the current reference and DCAP current injected into the grid. As shown in Fig.9, tracking seems to be appropriate.

Fig10 shows the current flowing through the grid, which is in phase with the grid voltage, i.e. only the active current is drawn from the grid, and reactive current and load harmonics are compensated simultaneously by DCAP. As shown in Fig.11, the THD value of grid current is reduced to 3.90% by DCAPs̀ model predictive control method while the THD value of the grid current is reduced to 7% by DCAPs̀ EHM/VQS method. Also, the power factor is increased from 0.89 to 0.999 in both methods. By comparing the results of EHM/VQS and MPC methods, the THD value is lower in the MPC method. As demon strated in Fig.12, at time t=t_1, a dynamic capacitor enters the circuit, and one inductive load at the time t=t_2 enters the circuit. As shown in Fig.12 and Fig.13, DCAP responds dynamically to load changes.

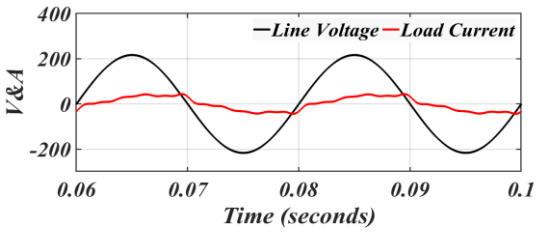

(a)

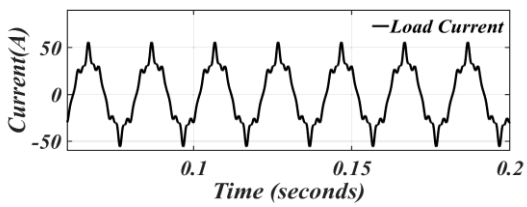

(b)

Fig.7 (a) Grid voltage and load current (b) Load current

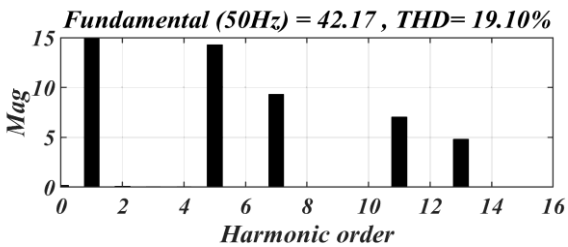

Fig.8 Load current THD

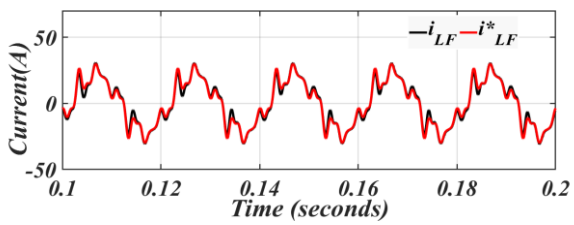

Fig.9 Reference current and DCAP

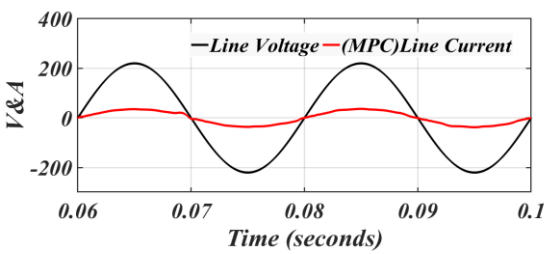

(a)

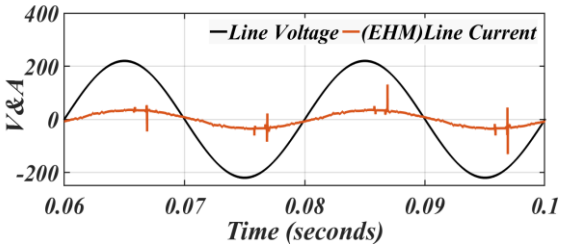

(b)

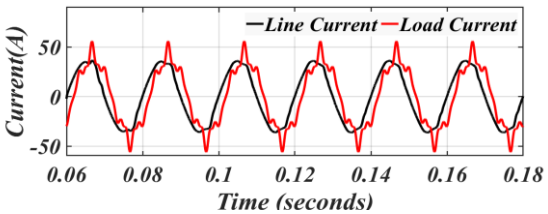

(c)

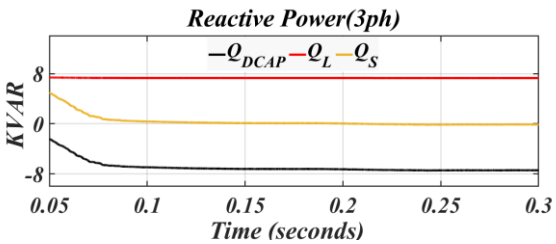

(d)

Fig10. (a) Voltage and current of the grid in the presence of the
DCAP with MPC method (b) Voltage and current of the grid in the presence of the DCAP with EHM method (c) Current of the grid and load in the presence of DCAP with MPC method (d) Reactive power

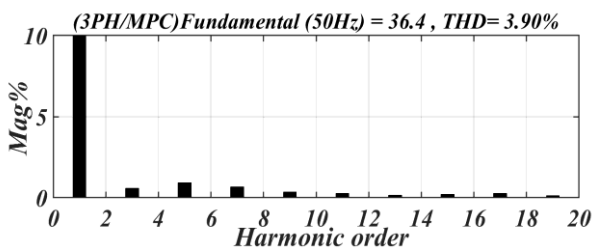

(a)

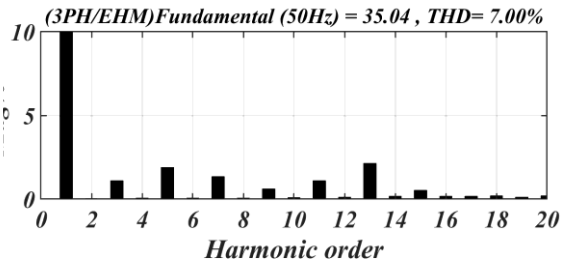

(b)

Fig.11 THD grid current in the presence of DCAP (a) MPC method (b) EHM method

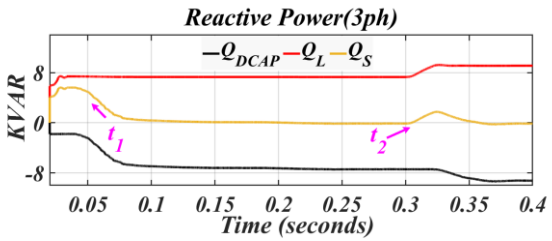

Fig.12 Reactive power

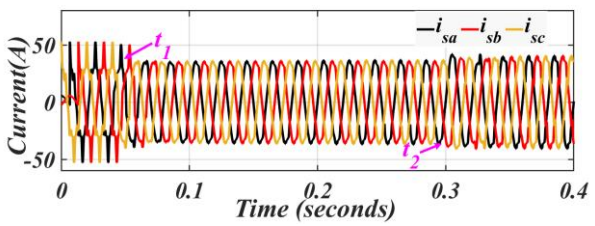

(a)

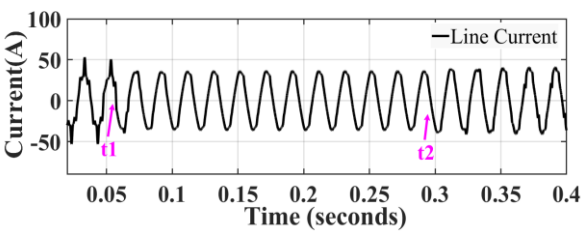

(b)

Fig.13 (a) and (b) current of the grid

4.2. Case 2

In this study, the performance of dynamic capacitors was assessed in the presence of even harmonics. Load current was lag and had odd and even harmonics up to 13, and THD grid current was equal to 20.41 while, power factor was poor (0.89).

Fig.14 and

Fig.15 show load current and content of its harmonics, respectively.

Fig.16 shows the current flowing through the grid, which is in phase with voltage meaning that active

current is drawn from the grid, and reactive current, and load harmonics are compensated simultaneously by DCAP. As shown in Fig17, the THD value of the grid current is reduced to 4.22% by the MPC method while the THD value of the grid current is reduced to 15.16 % by the EHM/VQS method indicating its inefficiency in filtering even-order harmonics. Also, in both methods, the power factor is increased from 0.89 to 0.999.

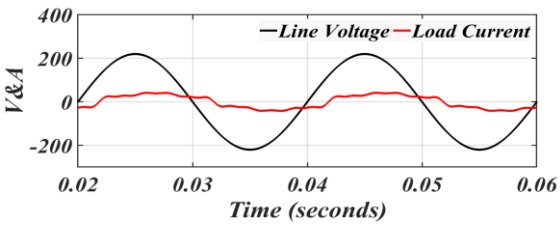

Fig.14 Grid voltage and load current

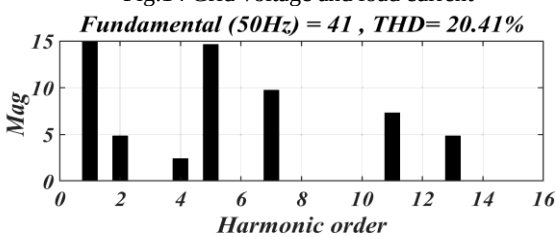

Fig.15. Load current THD

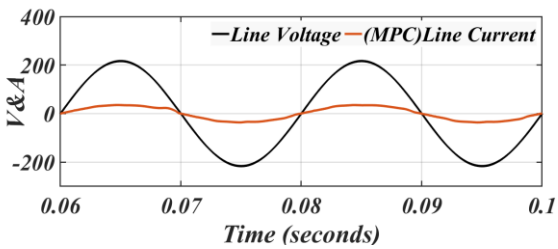

(a)

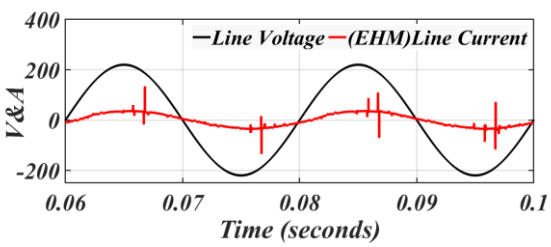

(b)

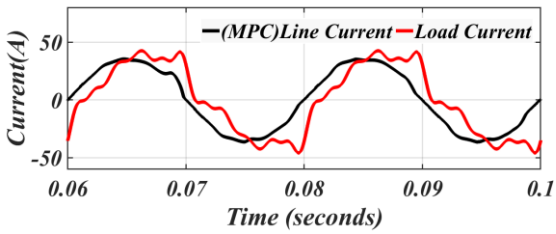

(c)

Fig.16 (a) Voltage and current of the grid in the presence of DCAP with MPC method (b) Voltage and current of the grid in the presence of DCAP with EHM method (c) Current of the grid and load in the presence of the DCAP with MPC method.

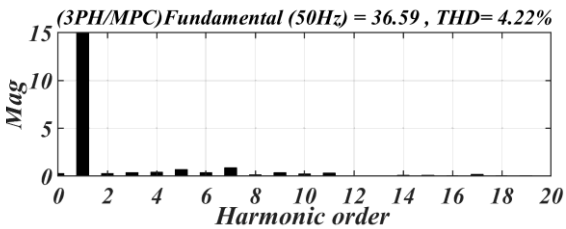

(a)

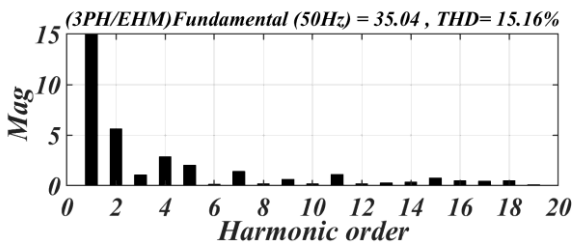

(b)

Fig17. THD grid current in the presence of DCAP (a) MPC method (a) EHM method

Therefore, the MPC method performs better than the EHM method in filtering even-order harmonics. Our results showed that the proposed method is not limited to even or odd types of harmonics, but it filters all the harmonics, and this type of ability does not exist in the EHM method.

4.3. Case 3

When the three-phase buck-type D-CAP is not used, THD of PCC voltage vT and grid current iS are obtained as shown in Fig.18 PCC voltage v_T and grid current i_S are seriously damaged, whose THD is equal to 3.61 and 19.31%, respectively. Finally, the three-

phase buck-type DCAP is applied for reactive compensation and harmonic suppression. As shown in Fig.19 and Fig.20, the THD value of the grid current is reduced to 3.91% by the model predictive control method when PCC voltage is harmonic, while the THD value of the grid current is reduced to 18.15% by the EHM method. This method does not work well in situations where the PCC voltage v_T is harmonic. Therefore, the MPC method performs better than the EHM method in these conditions. Our results indicated that the proposed method is not influenced by the harmonic voltage of the grid and the reference current changes according to harmonic conditions of the grid voltage, so the current injected by the DCAP will also change, which is not observed in the EHM method.

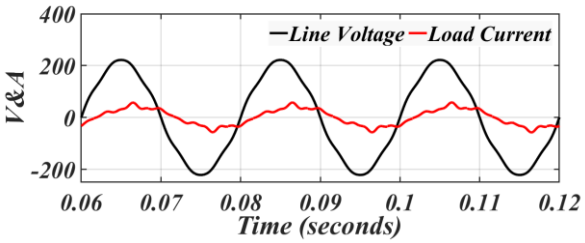

(a)

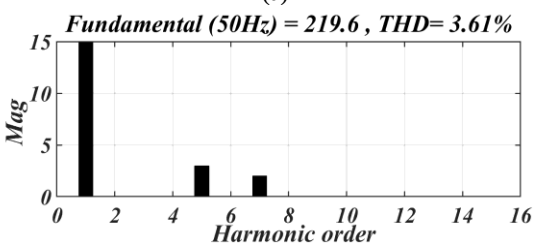

(b)

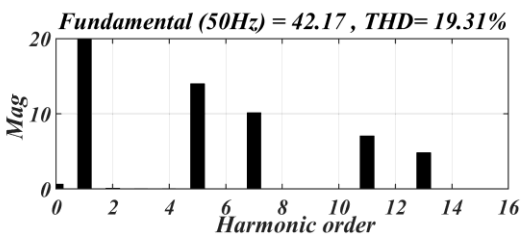

(c)

Fig.18 (a) Grid voltage and load current (b)THD grid voltage (c)THD grid current without the presence of DCAP.

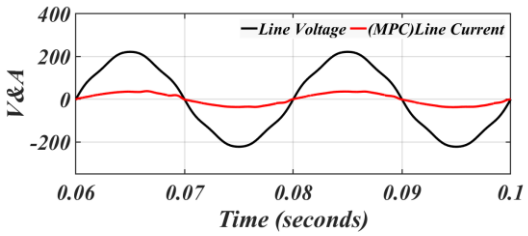

(a)

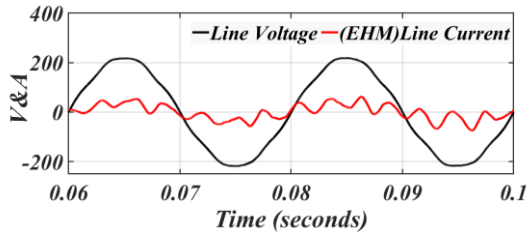

(b)

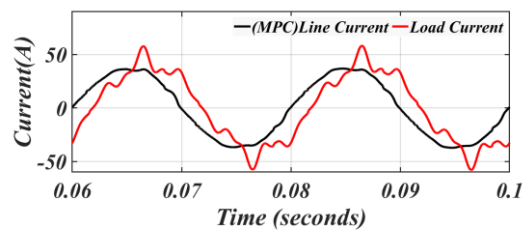

(c)

Fig.19 (a) Voltage and current of the grid in the presence of DCAP with MPC method (b) Voltage and current of the grid in the presence of DCAP with EHM method (c) Current of the grid and load in the presence of DCAP with MPC method.

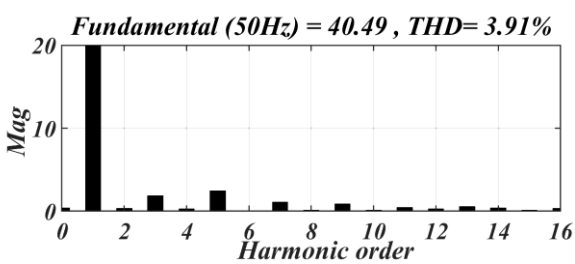

(a)

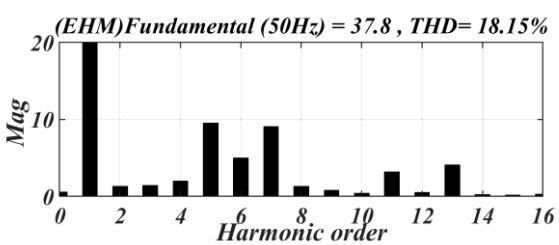

(b)

Fig.20 (a)THD grid current in the presence of DCAP using MPC method (b) THD grid current in the presence of DCAP using EHM method.

Table 3 compares the MPC method with the PI control method using the EHM/VQS concept in several indexes. Coupling Effect Index is referred to the effects of adjusting each harmonic control loop at any frequency on other control loops at other frequencies.

Table3. Comparison of control methods

Method / Index	EHM			MPC		
	case 1	case 2	case 3	case 1	case 2	case 3
power Factor	0.999	0.99	0.99	0.999	0.999	0.999
Current THD	7.00%	15.16%	18.15%	3.90%	4.22%	3.91%
Method	virtual quadrature sources/modulation			Predicting and tracking reference current		
Coupling effect	yes			no		
Frequency dependence	yes			no		
Complexity and limitations	High			Low		
Model	Approximate			exact		
Switching frequency	Fixed			Variable		
Dependence on the modulator	yes			no		
Ability to filter even harmonics	no			yes		
Affected by harmonic grid voltage	yes			no		

4.4. The effect of noise measurement on the performance and accuracy of the MPC method

This section describes the effect of measurement noise on the performance and accuracy of the MPC method. A basic and generally accepted noise model is known as Additive White Gaussian Noise (AWGN), which imitates various random processes seen in nature [29]. So the AWGN added to the current and voltage measured output used to MPC algorithm.

Fig.21 shows the performance for 10% of noise disturbance introduced in the current measures, that system performance is diminished compared with Fig.9, but the THD value is less than 5%. Thus, for the measured noise up to 10%, the proposed MPC robustness is good.

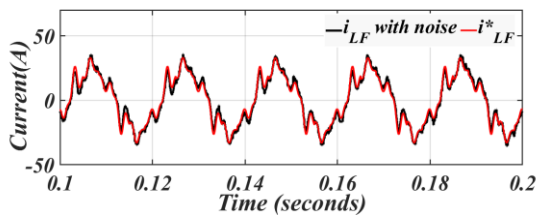

(a)

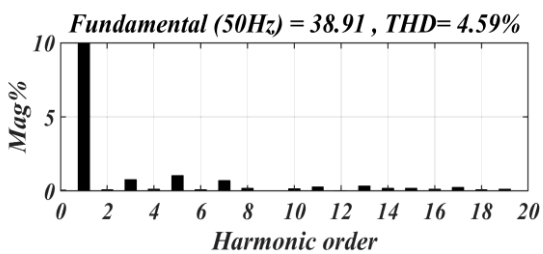

(b)

Fig.21 Performance for a 10% of noise disturbance introduced in the current measures (a) Output and reference current. (b) THD of grid current

5. CONCLUSION

In this paper, a new MPC -based control method was proposed for a three-phase three-wire buck-type DCAP, that as a shunt power quality device, corrects the power factor of the load and reduces the total harmonic distortion (THD) of the source current. Conventional EHM methods need to have harmonics contents and one PLL for each harmonic, and only works for odd harmonics, but the proposed MPC doesn't have these limitations. Also, switching signals are calculated directly without the need for a pulse-width modulation (PWM) scheme. The reference current consisted of two distinct parts, i.e., reactive

power compensator (RPC), and harmonic current eliminator (HCE), based on the fundamental component of the load current. Also, a prediction model contains all DCAP components was proposed to calculate state variables of the DCAP based on their previous values, state of the switches, and prediction values of the grid voltage. Simulation results showed the robustness of the proposed method against source voltage harmonic and different odd and even harmonic components in the load current. The proposed MPC method reduced the THD of the current source by more than 37% compared with the EHM method. The simulation results showed that the proposed method isn't affected by the grid voltage harmonic and is not limited to odd harmonics and filters all the harmonics that this ability does not exist in the EHM method. Also, for the measured noise up to 10%, the proposed MPC robustness is good.

APPENDIX

Values of each of the state variables at time *k* according to inputs of $v_{S,k}$ and S_k, and values of state variables at time *k-1* according to (A1) to (A4) are calculated by solving the system of 8 equations with 8 non-linear unknowns expressed in Equations (9) - (16) using the Symbolic math tool of the MATLAB software:

$$\begin{aligned} i_{LF,k} = (&C_F\Delta t^3 v_{S,k} - C_F\Delta t^3 v_{CF,k-1} - C\Delta t^3 S_k v_{C,k-1} + C\Delta t^3 S_k v_{S,k} - CC_F\Delta t^2 R_{LB} v_{CF,k-1} + C\Delta t^2 L_B S_k i_{LB,k-1} + C\Delta t^2 L_F S_k i_{LF,k-1} \\ &+ C_F\Delta t^2 L_F i_{LF,k-1} + CC_F\Delta t^2 R_{LB} v_{S,k} - CC_F\Delta t L_B v_{CF,k-1} + CC_F\Delta t L_F R_{LB} i_{LF,k-1} + CC_F\Delta t L_B v_{S,k} + CC_F L_B L_F i_{LF,k-1}) / A \end{aligned} \quad \text{(A1)}$$

$$\begin{aligned} i_{LB,k} = &C(\Delta t^2 L_B i_{LB,k-1} - \Delta t^3 v_{C,k-1} + \Delta t^3 S_k v_{S,k} + \Delta t^2 L_F S_k i_{LF,k-1} + C_F\Delta t^2 R_{LF} S_k v_{CF,k-1} - C_F\Delta t^2 R_{LF} v_{C,k-1} + C_F\Delta t L_F S_K v_{CF,k-1} \\ &+ C_F\Delta t L_B R_{LF} i_{LB,k-1} - C_F\Delta t L_F v_{C,k-1} + C_F L_B L_F i_{LB,k-1}) / A \end{aligned} \quad \text{(A2)}$$

$$\begin{aligned} v_{CF,k} = &(\Delta t^4 v_{S,k} + \Delta t^3 L_F i_{LF,k-1} + C_F\Delta t^3 R_{LF} v_{CF,k-1} + C\Delta t^3 R_{LF} S_k v_{C,k-1} + C\Delta t^3 R_{LB} v_{S,k} + C\Delta t^2 L_B v_{S,k} + CC_F\Delta t^2 R_{LB} R_{LF} v_{CF,k-1} \\ &+ C_F\Delta t^2 L_F v_{CF,k-1} - C\Delta t^2 L_B R_{LF} S_k i_{LB,k-1} + C\Delta t^2 L_F R_{LB} i_{LF,k-1} + C\Delta t^2 L_F S_k v_{C,k-1} - C\Delta t L_B L_F S_k i_{LB,k-1} + C\Delta t L_B L_F i_{LF,k-1} \\ &+ CC_F\Delta t L_F R_{LB} v_{CF,k-1} + CC_F\Delta t L_B R_{LF} v_{CF,k-1} + CC_F L_B L_F v_{CF,k-1}) / A \end{aligned} \quad \text{(A3)}$$

$$\begin{aligned} v_{C,k} = &(\Delta t^4 S_k v_{S,k} + \Delta t^3 L_B i_{LB,k-1} + C_F\Delta t^3 R_{LF} S_k v_{CF,k-1} + C\Delta t^3 R_{LF} S_k v_{C,k-1} + \Delta t^3 L_F S_k i_{LF,k-1} + C\Delta t^3 R_{LB} v_{C,k-1} + C\Delta t^2 L_F S_k v_{C,k-1} \\ &+ CC_F\Delta t^2 R_{LB} R_{LF} v_{C,k-1} + C_F\Delta t^2 L_B R_{LF} i_{LB,k-1} + C_F\Delta t^2 L_F S_k v_{CF,k-1} + C\Delta t^2 L_B v_{C,k-1} + C_F\Delta t L_B L_F i_{LB,k-1} + CC_F\Delta t L_B R_{LF} v_{C,k-1} \\ &+ CC_F\Delta t L_F R_{LB} v_{C,k-1} + CC_F L_B L_F v_{C,k-1}) / A \end{aligned} \quad \text{(A4)}$$

$$\begin{aligned} A = &\Delta t^4 + C\Delta t^2 L_B + C\Delta t^3 R_{LB} + C_F\Delta t^3 R_{LF} + C\Delta t^3 R_{LF} S_k + C_F\Delta t^2 L_F + C\Delta t^2 L_F S_k + CC_F\Delta t^2 R_{LB} R_{LF} + CC_F\Delta t L_B R_{LF} \\ &+ CC_F\Delta t L_F R_{LB} + CC_F L_B L_F \end{aligned}$$

REFERENCES

1. Fujita, H. and H. Akagi, *Voltage-Regulation Performance of a Shunt Active Filter Intended for Installation on a Power Distribution System.* IEEE Transactions on Power Electronics, 2007. **22**(3): p. 1046-1053.
2. Majumder, R., *Reactive Power Compensation in Single-Phase Operation of Microgrid.* IEEE Transactions on Industrial Electronics, 2013. **60**(4): p. 1403-1416.
3. *IEEE Guide for the Application of Shunt Power Capacitors.* IEEE Std 1036-2010 (Revision of IEEE Std 1036-1992), 2011: p. 1-88.
4. Prasai, A., J. Sastry, and D. Divan. *Dynamic Var/Harmonic Compensation with Inverter-Less Active Filters*. in *2008 IEEE Industry Applications Society Annual Meeting*. 2008.
5. Dijkhuizen, F. and M. Gödde. *Dynamic capacitor for HV applications*. in *2010 IEEE Energy Conversion Congress and Exposition*. 2010.
6. Morello, S., T.J. Dionise, and T.L. Mank, *Installation, Startup, and Performance of a Static VAR Compensator for an Electric Arc Furnace Upgrade.* IEEE

Transactions on Industry Applications, 2017. **53**(6): p. 6024-6032.
7. Mendoza-Araya, P., et al., *Lab-Scale TCR-Based SVC System for Educational and DG Applications.* IEEE Transactions on Power Systems, 2011. **26**(1): p. 3-11.
8. Song, Q., W. Liu, and Z. Yuan, *Multilevel Optimal Modulation and Dynamic Control Strategies for STATCOMs Using Cascaded Multilevel Inverters.* IEEE Transactions on Power Delivery, 2007. **22**(3): p. 1937-1946.
9. Singh, B. and J. Solanki, *A Comparison of Control Algorithms for DSTATCOM.* IEEE Transactions on Industrial Electronics, 2009. **56**(7): p. 2738-2745.
10. H. M, P. and M.T. Bina, *A Transformerless Medium-Voltage STATCOM Topology Based on Extended Modular Multilevel Converters.* IEEE Transactions on Power Electronics, 2011. **26**(5): p. 1534-1545.
11. Wheeler, P.W., et al., *Matrix converters: a technology review.* IEEE Transactions on Industrial Electronics, 2002. **49**(2): p. 276-288.
12. Raghuram, M., A.K. Chauhan, and S.K. Singh. *Switched capacitor impedance matrix converter*. in *2017 IEEE Energy Conversion Congress and Exposition (ECCE)*. 2017.
13. Akagi, H., *Active Harmonic Filters.* Proceedings of the IEEE, 2005. **93**(12): p. 2128-2141.
14. Zhao, W., et al. *Injection-type hybrid active power filter in high-power grid with background harmonic voltage*. IET Power Electronics, 2011. **4**, 63-71.
15. Prasai, A., J. Sastry, and D.M. Divan, *Dynamic Capacitor (D-CAP): An Integrated Approach to Reactive and Harmonic Compensation.* IEEE Transactions on Industry Applications, 2010. **46**(6): p. 2518-2525.
16. Prasai, A. and D.M. Divan, *Control of Dynamic Capacitor.* IEEE Transactions on Industry Applications, 2011. **47**(1): p. 161-168.
17. Divan, D.M. and J. Sastry, *Voltage Synthesis Using Dual Virtual Quadrature Sources—A New Concept in AC Power Conversion.* IEEE Transactions on Power Electronics, 2008. **23**(6): p. 3004-3013.
18. Wu, W., S. Xie, and J. Cao. *Topology and control strategy design for AC chopper based VAR compensators*. in *2013 IEEE ECCE Asia Downunder*. 2013.
19. Chen, X., et al. *Reactive power compensation with improvement of current waveform quality for single-phase buck-type Dynamic Capacitor*. in *2016 IEEE Applied Power Electronics Conference and Exposition (APEC)*. 2016.
20. Wu, Q., et al., *Reactive Current Reshaping With Series Resonance Damping for Three-Phase Buck-Type Dynamic Capacitor.* IEEE Access, 2019. **7**: p. 142663-142674.
21. Wang, X., et al., *Reactive Power Compensation and Imbalance Suppression by Star-Connected Buck-Type D-CAP*. Energies, 2019. **12**(10): p. 1914.
22. Wang, X., et al. *Optimal Compensation of Delta-connected Dynamic Capacitor for Unbalanced Load*. in *2018 IEEE International Power Electronics and Application Conference and Exposition (PEAC)*. 2018.
23. Chao, Z., et al., *Series and parallel resonance active damping of three-phase buck-type dynamic capacitor for reactive compensation and harmonic suppression.* IET Power Electronics, 2020.
24. Chen, X., et al. *Interaction and coordination between reactive compensation and harmonic suppression for three-phase buck-type D-CAP*. IET Power Electronics, 2019. **12**, 2953-2964.
25. Karamanakos, P., et al., *Direct Model Predictive Control: A Review of Strategies That Achieve Long Prediction Intervals for Power Electronics.* IEEE Industrial Electronics Magazine, 2014. **8**(1): p. 32-43.
26. Bordons, C. and C. Montero, *Basic Principles of MPC for Power Converters: Bridging the Gap Between Theory and Practice.* IEEE Industrial Electronics Magazine, 2015. **9**(3): p. 31-43.
27. Hamidi, S.S. and H. Gholizade-Narm, *Power injection of renewable energy*

sources using modified model predictive control. Energy Equipment and Systems, 2016. **4**(2): p. 215-224.

28. Lin, M., et al., *FCS-MPC control strategy for a new fault tolerant three-level inverter*. automatika, 2016. **57**(3): p. 589-598.
29. Vazquez, S., et al. *Model predictive control of a VSI with long prediction horizon*. in *2011 IEEE International Symposium on Industrial Electronics*. 2011. IEEE.